HHS Public Access

Author manuscript

Magn Reson Med. Author manuscript; available in PMC 2015 October 20.

Published in final edited form as:

Magn Reson Med. 2015 August ; 74(2): 544–549. doi:10.1002/mrm.25748.

Tumor-Specific Expression and Detection of a CEST Reporter Gene

Il Minn[1], **Amnon Bar-Shir**[1,2], **Keerthi Yarlagadda**[1], **Jeff W. M. Bulte**[1,2], **Paul B. Fisher**[3,4,5], **Hao Wang**[6], **Assaf A. Gilad**[1,2], and **Martin G. Pomper**[1,7,*]

[1]The Russell H. Morgan Department of Radiology and Radiological Science, The Johns Hopkins University School of Medicine, Baltimore, Maryland, USA.

[2]Cellular Imaging Section, Institute for Cell Engineering, The Johns Hopkins University School of Medicine, Baltimore, Maryland, USA.

[3]Department of Human and Molecular Genetics, Virginia Commonwealth University, Richmond, Virginia, USA.

[4]VCU Institute of Molecular Medicine, Virginia Commonwealth University, Richmond, Virginia, USA.

[5]VCU Massey Cancer Center, Virginia Commonwealth University, Richmond, Virginia, USA.

[6]Division of Biostatistics and Bioinformatics, The Johns Hopkins University, Baltimore, Maryland, USA

[7]Sidney Kimmel Comprehensive Cancer Center, The Johns Hopkins University, Baltimore, Maryland, USA

Abstract

Purpose—To develop an imaging tool that enables the detection of malignant tissue with enhanced specificity using the exquisite spatial resolution of MRI.

Methods—Two mammalian gene expression vectors were created for the expression of the lysine-rich protein (LRP) under the control of the cytomegalovirus (CMV) promoter and the progression elevated gene-3 promoter (PEG-3 promoter) for constitutive and tumor-specific expression of LRP, respectively. Using those vectors, stable cell lines of rat 9L glioma, $9L^{CMV\text{-}LRP}$ and $9L^{PEG\text{-}LRP}$, were established and tested for CEST contrast *in vitro* and *in vivo*.

Results—$9L^{PEG\text{-}LRP}$ cells showed increased CEST contrast compared with 9L cells *in vitro*. Both $9L^{CMV\text{-}LRP}$ and $9L^{PEG\text{-}LRP}$ cells were capable of generating tumors in the brains of mice, with a similar growth rate to tumors derived from wild-type 9L cells. An increase in CEST contrast was clearly visible in tumors derived from both $9L^{CMV\text{-}LRP}$ and $9L^{PEG\text{-}LRP}$ cells at 3.4 ppm.

*Correspondence to: Martin G. Pomper, M.D., Ph.D., Johns Hopkins Medical School, 1550 Orleans Street, 492 CRB II, Baltimore, MD 21287-0014. mpomper@jhmi.edu.

Conclusion—The PEG-3 promoter:LRP system can be used as a cancer-specific, molecular-genetic imaging reporter system *in vivo*. Because of the ubiquity of MR imaging in clinical practice, sensors of this class can be used to translate molecular-genetic imaging rapidly.

Keywords

molecular imaging; chemical exchange saturation transfer; PEG-3 promoter; glioma; magnetic resonance imaging

INTRODUCTION

Molecular-genetic MRI uses reporter-imaging probe pairs that can generate MR contrast (1). The goal of molecular-genetic MRI is to leverage the superior three-dimensional spatial resolution of MRI to develop reporter-based, targeted MRI systems. Many reporters have been identified as candidate MR contrast-generating genes. Those include: the β-galactosidase-Gd^{3+}-containing galactopyranosyl ring reporter-probe pair for T_1 contrast (2); the tyrosinase-paramagnetic iron pair for T_2 contrast (3); the transferrin receptor-monocrystalline iron oxide nanocompound pair for T_2 contrast (4); the ferritin and endogenous iron pair for T_2 contrast (5,6); the Mag A-iron pair for T_2 contrast (7); and, the secreted alkaline phosphatase (SEAP)-phospho-rylated metalloporphyrin pair for T_1 contrast (8). We have developed an artificial gene, the lysine-rich protein (LRP), as a reporter for chemical exchange saturation transfer (CEST) MRI (9). The LRP provides a high density of amide protons, which enables detection by MRI without requiring administration of a cognate probe. LRP-expressing tumors in the mouse brain have been imaged by CEST MRI (9).

For imaging reporter genes to be applied in a target-specific manner, they should either be delivered exclusively to their targets or expressed specifically within the target cells. The latter can be accomplished by using a target-selective promoter to drive the expression of a reporter following systemic delivery of a reporter plasmid. Many promoters of genes with elevated expression in human cancers have been examined as potential cancer-specific promoters, but most are active only in cancers of certain tissues of origin (10,11). The optimal promoters for cancer-specific, molecular-genetic imaging would be active in a variety of human cancers, while remaining minimally active or silent in normal tissues. We have identified a minimal promoter from a rodent gene, the progression elevated gene-3 (PEG-3 promoter), through subtraction hybridization while searching for genes involved in malignant transformation and tumor progression (12). We found that the PEG-3 promoter behaves as a cancer-specific promoter as it is active in a variety of human cancers, including brain, prostate, breast, pancreatic, and skin cancers, with minimal activity in normal counterpart tissues (13–16). Tumor specificity of the PEG-3 promoter has been attributed to binding sites of two transcription factors, AP-1 and PEA-3 (or E1AF, the human homolog), which are reported to be overexpressed in human cancer cells (13). Systemic delivery of the PEG-3 promoter-reporter plasmid followed by imaging with bioluminescence or single photon emission computed tomography (SPECT) enabled detection of micrometastases in experimental models of human breast cancer and melanoma (17). However, bioluminescence imaging cannot extend beyond preclinical models and SPECT is fraught

with relatively low spatial resolution. Accordingly we turned to MRI with the PEG-3 promoter to drive production of LRP in a cancer-specific manner with the high spatial resolution of this modality.

The LRP is based on CEST, a relatively new MR contrast mechanism (18–20). CEST allows detection of bioorganic molecules, such as proteins (21,22), polysaccharides (23,24), metabolites (25–27), enzyme substrates (28–31) as well as injectable compounds (32) due to the exchange of MR-saturable, labile protons in these molecules with those of water. Here, we present a molecular-genetic imaging approach to detect tumor-specific gene expression in an animal model of glioma by using the MR reporter gene LRP and CEST MRI. The LRP was expressed under control of the tumor-specific PEG-3 promoter in rat 9L glioma cells ($9L^{PEG\text{-}LRP}$). $9L^{PEG\text{-}LRP}$ cells transplanted to a mouse brain showed higher CEST contrast compared with that from similarly transplanted wild-type cells. Our results demonstrate the feasibility of using a CEST-based reporter gene under a tumor-specific promoter for detection of tumors in vivo with MRI.

METHODS

In Vitro Assessment of PEG-Promoter Activity

The dual-luciferase assay was carried out to measure promoter activities in rat 9L glioma cells. 9L cells were grown in RPMI 1640 supplemented with 10% fetal bovine serum and 1× penicillin and streptomycin in a humidified incubator (37°C, 5% CO_2). 9L cells were seeded in 24-well plates (1×10^5 cells per well). Forty-eight hours later, cells were transiently transfected with the following combination of plasmids using jetPRIME® according to the manufacturer's instructions (Polyplus-Transfection Inc., Illkirch, France); (i) pPEG-Luc (17) + pGL4.74 (Promega, Madison, WI), (ii) pCMV-Tri (17) + pGL4.74, and (iii) pGL3-basic (Promega, Madison WI) + pGL4.74 with a 10:1 ratio for each preparation. pPEG-Luc possess PEG-3 promoter driven firefly luciferase (fLuc), pCMV-Tri has CMV promoter driven fLuc, and pGL3-basic plasmid has no promoter, serving as a promoterless control. pGL4.74 plasmid expresses Renilla luciferase (rLuc) to normalized the transfection efficiency. At 48 h post-transfection, fLuc activity was measured using the Dual-Luciferase® Reporter Assay System (Promega). The fLuc activity was normalized to rLuc activity and total protein amount measured by the Coomasie® protein assay reagent kit (Pierce Biotechnology, Rockford, IL).

Cloning of the Expression Constructs

The pMONO-neo-mcs vector was purchased from InvivoGen (San Diego, CA) and the ferritin heavy chain core promoter was replaced with the PEG-3 promoter to create pPEG-neo-mcs. Lysine-rich protein (LRP), which consists of four repeats of 'MGKKKKKKKKKKKKKKKKKKKKKKKKGS' and a V5 tag, was amplified by polymerase chain reaction (PCR) using pLRP101 (9) as a template and inserted into pPEG-neo-msc and pCEP4 (Life Technologies, Carlsbad, CA) to create pPEG-LRP and pCMV-LRP, respectively. The sequence of the vector was confirmed (MacrogenUSA, Rockville, MD). Primers used for PCR were as follows: PEG-3 Promoter for pPEG-neo-msc (Forward: CAGAACTAGTAGAAAGAGAAAGAGAATGGGAC; Reverse: AAC

AGGATCCGTCCGGTTCGGTTTGC CAAAAGCG), LRP for pPEG-LRP (Forward: CTAAATCG ATCCATCATTTGTACAAAAAAGCAGGCTCCG; Reverse: AGCACCTAGGTTACTAACCGGTACGCGTAGAATCGAG), LRP for pCMV-LRP (Forward: CAGTAAGCTTCCATCAT TTGTACAAAAAAGCAGGCTCCG; Reverse: CACAATCTC GAGTTAC TAACCGGTACGCGTAGAATCGAG).

Establishing a Stable Cell Line Expressing pPEG-LRP and pCMV-LRP

9L cells were transfected separately with pPEG-LRP and pCMV-LRP using Lipofectamine 2000 (Life Technologies, Carlsbad, CA) according to the manufacturer's instructions. $9L^{PEG\text{-}LRP}$ and $9L^{CMV\text{-}LRP}$ were selected by maintaining cells after the transfection in growth medium containing 1 mg/mL of G-418 (Life Technologies, Carlsbad, CA) and 100 μg/mL of Hygromycin B (Corning Cell-gro, Manassas, VA), respectively.

In Vitro CEST MRI

In vitro CEST MRI experiments were performed as previously described (33,34) with the following modifications. In brief, 1×10^7 cells were placed in a 5 mm NMR tube (three tubes from three separate preparations, for each cell type, 9L or $9L^{PEG\text{-}LRP}$) and placed within a vertical-bore 11.7T Bruker Avance system (Bruker Biosciences Corp., Billerica, MA) at 37°C. A modified RARE (repetition time/echo time [TR/TE] = 5000/20 ms, RARE factor = 8, 1 mm slice thickness, field of view (FOV) = 1.7 × 1.7 cm, matrix size = 128 × 64, resolution = 0.17 × 0.34 mm, and NA = 2) sequence, including a magnetization transfer (MT) module (B_1 = 3.6 μT/3000 ms) was used to acquire CEST weighted images from −4.4 ppm to +4.4 ppm (step = 0.2 ppm) around the water resonance (0 ppm). For B_0 shift correction of each pixel in the CEST image, the absolute water resonant frequency shift was measured using a modified Water Saturation Shift Reference (WASSR) method (35), using the same parameters as in CEST imaging except TR = 1500 ms, saturation pulse of 500 ms, B1 = 0.5 μT and a sweep range from −1 ppm to 1 ppm (step = 0.1 ppm).

Animal Model

NOD/SCID/IL2rγ^{null} (NSG) mice were purchased from the Animal Resource Core of the Sidney Kimmel Comprehensive Cancer Center of Johns Hopkins. Mice were anaesthetized by inhaling 1.5% isoflurane/oxygen gas. Small holes were made on the skull at 2 mm lateral to the bregma. 2×10^5 cells in 2 μL of media were directly injected into the striatum 3 mm deep from the skull using a 24 gauge Hamilton syringe over 5 min. Animal experiments were performed in accordance with protocols approved by Johns Hopkins Animal Care and Use Committee (ACUC).

In Vivo CEST MRI

Mice with bilateral tumors within striatum (9L and $9L^{PEG\text{-}LRP}$, n = 8) and (9L and $9L^{CMV\text{-}LRP}$, n = 1) were used. Data were acquired using a horizontal-bore 11.7 Tesla (T) MRI scanner (Bruker Biospec) equipped with a circular polarized MRI transceiver coil (ID = 23 mm). Seven days after cell transplantation, mice were anesthetized with 1.5% isoflurane and CEST data were obtained as previously described (33,36), and with the following parameters: A single 1 mm slice with FOV of 1.6×1.6 cm^2 and a 96 × 48 matrix

were used, resulting in an in-plane resolution of 0.167 × 0.333 mm. CEST-weighted images were acquired with a modified RARE pulse sequence (TR/TE = 6000/35 ms), using a 3.6 μT/3000 ms saturation pulse from −4.2 to +4.2 ppm (0.2 ppm steps) around the water resonance, which was assigned to be at 0 ppm (total experimental time of 41 min). Pixel-based B_0 correction was used as described before (35) using the same parameters as above except for TR = 1500 ms, B_1/t_{sat} = 0.5 μT/500 ms, with a sweep range from −1 to +1 ppm (0.1 ppm steps). Mean CEST spectra (Z-spectra) were plotted from a region of interest (ROI) for each tumor and normal brain tissue, after B_0 correction.

CEST Data Processing

Data processing was performed using custom-written scripts in Matlab as described earlier (33). Mean Z-spectra were used from a ROI for each sample, after B_0 correction for each voxel. $MTR_{asym} = 100 \times (S^{-\Delta\omega} - S^{\Delta\omega})/S^0$ was computed at different offsets, Δω. To remove magnetization transfer effects, ΔMTR_{asym} was defined as $[MTR_{asym}$ (tumor)] – $[MTR_{asym}$ (normal brain tissue)], as previously described (37).

Statistical Analyses

Because a series of frequencies was applied to the same sample in the *in vitro* CEST MRI, the generalized estimating equation (GEE) approach (38) was used to take into account the correlations across the frequencies when we compared the CEST contrast in 9L and $9L^{PEG\text{-}LRP}$ cells, and *P* values of the score test were reported. The GEE method was also applied to the comparisons in the *in vivo* CEST MRI study to account for the correlations arising from the fact that paired data of 9L and $9L^{PEG\text{-}LRP}$ cells were collected from the same mouse and each was measured with a series of frequencies. All the tests were two-sided. The analysis was performed using software SAS (version 9.4, Cary, NC)

RESULTS

We first examined whether the PEG-3 promoter was active in the 9L cell line. After transient transfection of 9L cells with pGL3-basic (no promoter control), pPEG-Luc (17), and pCMV-Tri (17), we measured fLuc activity driven by each promoter. The PEG-3 promoter showed activity comparable to one third of that of the CMV promoter in 9L cells (Fig. 1).

To develop cell lines that stably express LRP, we created two mammalian expression vectors for constitutive (pCMV-LRP) and tumor-specific (pPEG-LRP) gene expression. The pCMV-LRP construct was equipped with the CMV promoter and the hygromycin B resistance gene. The pPEG-LRP construct was equipped with the tumor-specific PEG-3 promoter and the neomycin resistance gene. To enhance the relatively weak activity of the PEG-3 promoter compared with the CMV promoter (Fig. 1), an SV40 enhancer and an SV40 polyadenylation site were inserted upstream and downstream of the PEG-3 promoter:LRP construct, respectively. After transfecting rat 9L glioma cells with those vectors, we selected cells expressing LRP by maintaining them in media containing hygromycin B and G418 and used surviving cells ($9L^{CMV\text{-}LRP}$ and $9L^{PEG\text{-}LRP}$) for further study. We performed *in vitro* CEST MRI to test whether the LRP expressing cells generated

CEST contrast. $9L^{PEG\text{-}LRP}$ cells showed increased CEST contrast compared with 9L cells at 3.3–3.9 ppm, the frequency at which the original LRP generated contrast (9) (Fig. 2).

We then developed murine glioma models to test LRP *in vivo*. 9L, $9L^{CMV\text{-}LRP}$, and $9L^{PEG\text{-}LRP}$ cells were capable of forming tumors in the brains of immunocompromised NSG mice, as shown by T2-weighed MRI (Figs. 3a,c). An increase in CEST contrast was visible in tumors derived from both $9L^{CMV\text{-}LRP}$ and $9L^{PEG\text{-}LRP}$ cells compared with wild-type 9L tumors, as shown in Figs. 3b,d. We imaged a total of eight mice harboring 9L (left) and $9L^{PEG\text{-}LRP}$ (right) in the brain. The average CEST contrast, i.e., ΔMTR_{asym} value, was significantly higher ($P < 0.01$; n = 8) for tumors derived from cells expressing LRP than from the wild-type 9L tumors at 3.4 ppm (Figs. 3e,f). These results demonstrate that a CEST reporter gene can be expressed *in vivo* in a tumor-specific manner and can be used as a tumor-specific biomarker for MR applications.

DISCUSSION

In this preclinical study, we present proof-of-principle for cancer-specific CEST MRI using reporter-based, molecular-genetic imaging. Many reporter genes that produce MR contrast for imaging have been identified and have shown promising characteristics for MR-based molecular-genetic imaging (10,39,40). To apply those reporters to the clinic, they should be selectively expressed in target cells, namely, cancer. Targeted delivery and selective transfection of reporter plasmid is a challenging task, especially for small or micrometastatic lesions. Using a target-specific promoter to control the expression of a reporter at the target is an alternative approach, which we have chosen. The optimal promoter for cancer-specific imaging would be robustly active in a wide variety of human cancers, while remaining inactive or minimally active in normal tissue. We leveraged the well-studied, cancer-specific PEG-3 promoter to drive the expression of the synthetic CEST probe, LRP. We have shown that the PEG-3 promoter is active in all human cancer types tested and is minimally active in the corresponding normal tissues (8,9,12). Because the PEG-3 promoter originated from a rodent genome, and humans do not have the orthologous gene, there is very little possibility of unwanted chromosomal insertion through homologous recombination. In addition, the relatively small size of the PEG-3 promoter (465 base pairs) will be an advantage for designing smaller imaging vectors for improved transfection efficiency (41).

The LRP does not require additional administration of the probe because the amide protons from the lysine residue are the source of CEST contrast. PEG-3 promoter-driven LRP expression with the SV40 enhancer in animal models of glioma was sufficient to generate detectable CEST contrast.

We designed the pPEG-LRP vector to be suitable for systemic delivery and clinical translation. The vector has the clinically compatible kanamycin resistance marker for the production of the plasmid (42). Additionally, the pPEG-LRP has a small size of 3575 base pairs, which can enable enhanced transfection efficiency (41). The present study demonstrated limited CEST contrast from LRP, potentially due to weak promoter activity of tumor-specific PEG-3 promoter. Further modifications of the small pPEG-LRP plasmid to augment the expression of LRP would enhance the sensitivity of detection. For example, a

two-step transcriptional amplification system can be introduced to increase the number of LRP molecules expressed (11,43). Adding scaffold/matrix attachment regions (S/MARs) to the plasmid will enable prolonged maintenance of the plasmid, resulting in accumulation of LRP within the transfected cancer cells. Also, using longer LRP would enhance CEST contrast. Indeed, CEST imaging using traditional pulse sequences, as in this study, is limited by low sensitivity, manifested by only a few percent change in contrast, especially for biological samples. This is also true for the LRP. As shown above, only a small yet significant ($P < 0.01$) change was observed. In a similar case, where LRP was used to monitor Oncolytic Virotherapy (44), a significant change was detected; however, it was on the same order of magnitude as described here. Nevertheless, CEST is an evolving field of MRI and new techniques that can improve the sensitivity are constantly under development, including methods for isolating the CEST signal from rapidly exchanging protons such as through length and offset varied saturation (LOVRS) (45), frequency-labeled exchange (FLEX) (46) as well as through separation of the contrast from endogenous contrast from proteins or magnetization transfer contrasts (47).

The PEG-3 promoter:LRP system enabled cancer-specific imaging using CEST MR *in vivo* in the rat 9L glioma model. Efforts to extend those findings to experimental models of human cancer in the periphery, with a focus on systemic delivery of the plasmid to detect metastatic disease, are under way.

ACKNOWLEDGMENTS

We thank CA134675 (M.G.P.), CA058236; CA151838 (Johns Hopkins SPORE in Prostate Cancer); the A. David Mazzone Research Awards Program (M.G.P., P.B.F.), Maryland Stem Cell Research Fund, MSCRFII-0042 (A.A.G.), Maryland Stem Cell Research Fund, MSCRFF-0103-00 (A.B.S.), National Foundation for Cancer Research (P.B.F.) and CA134721 (P.B.F.). P.B.F. holds the Thelma Newmeyer Corman Chair in Cancer Research in the VCU Massey Cancer Center. We also thank Dr. M. McMahon for insightful discussions.

Grant sponsor: National Institutes of Health; Grant number: CA134675, CA058236; CA151838; CA134721; Grant sponsor: the A. David Mazzone Research Awards Program; Grant sponsor: Maryland Stem Cell Research Fund; Grant number: MSCRFII-0042, MSCRFF-0103-00; Grant sponsor: National Foundation for Cancer Research; Grant sponsor: National Cancer Institute.

REFERENCES

1. Gilad AA, Ziv K, McMahon MT, van Zijl PC, Neeman M, Bulte JW. MRI reporter genes. J Nucl Med. 2008; 49:1905–1908. [PubMed: 18997049]
2. Louie AY, Huber MM, Ahrens ET, Rothbacher U, Moats R, Jacobs RE, Fraser SE, Meade TJ. In vivo visualization of gene expression using magnetic resonance imaging. Nat Biotechnol. 2000; 18:321–325. [PubMed: 10700150]
3. Alfke H, Stoppler H, Nocken F, Heverhagen JT, Kleb B, Czubayko F, Klose KJ. In vitro MR imaging of regulated gene expression. Radiology. 2003; 228:488–492. [PubMed: 12801999]
4. Weissleder R, Moore A, Mahmood U, Bhorade R, Benveniste H, Chiocca EA, Basilion JP. In vivo magnetic resonance imaging of trans-gene expression. Nat Med. 2000; 6:351–355. [PubMed: 10700241]
5. Cohen B, Dafni H, Meir G, Harmelin A, Neeman M. Ferritin as an endogenous MRI reporter for noninvasive imaging of gene expression in C6 glioma tumors. Neoplasia. 2005; 7:109–117. [PubMed: 15802016]
6. Genove G, Demarco U, Xu H, Goins WF, Ahrens ET. A new transgene reporter for in vivo magnetic resonance imaging. Nat Med. 2005:450–454. [PubMed: 15778721]

7. Zurkiya O, Chan AW, Hu X. MagA is sufficient for producing magnetic nanoparticles in mammalian cells, making it an MRI reporter. Magn Reson Med. 2008; 59:1225–1231. [PubMed: 18506784]
8. Westmeyer GG, Emer Y, Lintelmann J, Jasanoff A. MRI-based detection of alkaline phosphatase gene reporter activity using a porphyrin solubility switch. Chem Biol. 2014; 21:422–429. [PubMed: 24613020]
9. Gilad AA, McMahon MT, Walczak P, Winnard PT Jr. Raman V, van Laarhoven HW, Skoglund CM, Bulte JW, van Zijl PC. Artificial reporter gene providing MRI contrast based on proton exchange. Nat Biotechnol. 2007; 25:217–219. [PubMed: 17259977]
10. Bhang HE, Pomper MG. Cancer imaging: gene transcription-based imaging and therapeutic systems. Int J Biochem Cell Biol. 2012; 44:684–689. [PubMed: 22349219]
11. Minn I, Menezes ME, Sarkar S, Yarlagadda K, Das SK, Emdad L, Sarkar D, Fisher PB, Pomper MG. Molecular-genetic imaging of cancer. Adv Cancer Res. 2014; 124:131–169. [PubMed: 25287688]
12. Su ZZ, Shi Y, Fisher PB. Subtraction hybridization identifies a transformation progression-associated gene PEG-3 with sequence homology to a growth arrest and DNA damage-inducible gene. Proc Natl Acad Sci U S A. 1997; 94:9125–9130. [PubMed: 9256446]
13. Su ZZ, Sarkar D, Emdad L, Duigou GJ, Young CS, Ware J, Randolph A, Valerie K, Fisher PB. Targeting gene expression selectively in cancer cells by using the progression-elevated gene-3 promoter. Proc Natl Acad Sci U S A. 2005; 102:1059–1064. [PubMed: 15647352]
14. Sarkar D, Su ZZ, Vozhilla N, Park ES, Randolph A, Valerie K, Fisher PB. Targeted virus replication plus immunotherapy eradicates primary and distant pancreatic tumors in nude mice. Cancer Res. 2005; 65:9056–9063. [PubMed: 16204080]
15. Sarkar D, Lebedeva IV, Su ZZ, Park ES, Chatman L, Vozhilla N, Dent P, Curiel DT, Fisher PB. Eradication of therapy-resistant human prostate tumors using a cancer terminator virus. Cancer Res. 2007; 67:5434–5442. [PubMed: 17545625]
16. Sarkar D, Su ZZ, Park ES, Vozhilla N, Dent P, Curiel DT, Fisher PB. A cancer terminator virus eradicates both primary and distant human melanomas. Cancer Gene Ther. 2008; 15:293–302. [PubMed: 18323853]
17. Bhang HE, Gabrielson KL, Laterra J, Fisher PB, Pomper MG. Tumor-specific imaging through progression elevated gene-3 promoter-driven gene expression. Nat Med. 2011; 17:123–129. [PubMed: 21151140]
18. Sherry AD, Woods M. Chemical exchange saturation transfer contrast agents for magnetic resonance imaging. Annu Rev Biomed Eng. 2008; 10:391–411. [PubMed: 18647117]
19. van Zijl PC, Yadav NN. Chemical exchange saturation transfer (CEST): what is in a name and what isn't? Magn Reson Med. 2011; 65:927–948. [PubMed: 21337419]
20. Yoo B, Pagel MD. An overview of responsive MRI contrast agents for molecular imaging. Front Biosci. 2008; 13:1733–1752. [PubMed: 17981664]
21. Zhou J, Payen JF, Wilson DA, Traystman RJ, van Zijl PC. Using the amide proton signals of intracellular proteins and peptides to detect pH effects in MRI. Nat Med. 2003; 9:1085–1090. [PubMed: 12872167]
22. Zhou J, Tryggestad E, Wen Z, et al. Differentiation between glioma and radiation necrosis using molecular magnetic resonance imaging of endogenous proteins and peptides. Nat Med. 2011; 17:130–134. [PubMed: 21170048]
23. van Zijl PC, Jones CK, Ren J, Malloy CR, Sherry AD. MRI detection of glycogen in vivo by using chemical exchange saturation transfer imaging (glycoCEST). Proc Natl Acad Sci U S A. 2007; 104:4359–4364. [PubMed: 17360529]
24. Ling W, Regatte RR, Navon G, Jerschow A. Assessment of glycosaminoglycan concentration in vivo by chemical exchange-dependent saturation transfer (gagCEST). Proc Natl Acad Sci U S A. 2008; 105:2266–2270. [PubMed: 18268341]
25. Chan KW, Liu G, Song X, et al. MRI-detectable pH nanosensors incorporated into hydrogels for in vivo sensing of transplanted-cell viability. Nat Mater. 2013; 12:268–275. [PubMed: 23353626]
26. Cai K, Haris M, Singh A, Kogan F, Greenberg JH, Hariharan H, Detre JA, Reddy R. Magnetic resonance imaging of glutamate. Nat Med. 2012; 18:302–306. [PubMed: 22270722]

27. Walker-Samuel S, Ramasawmy R, Torrealdea F, et al. In vivo imaging of glucose uptake and metabolism in tumors. Nat Med. 2013; 19:1067–1072. [PubMed: 23832090]
28. Liu G, Liang Y, Bar-Shir A, et al. Monitoring enzyme activity using a diamagnetic chemical exchange saturation transfer magnetic resonance imaging contrast agent. J Am Chem Soc. 2011; 133:16326–16329. [PubMed: 21919523]
29. Airan RD, Bar-Shir A, Liu G, Pelled G, McMahon MT, van Zijl PC, Bulte JW, Gilad AA. MRI biosensor for protein kinase A encoded by a single synthetic gene. Magn Reson Med. 2012; 68:1919–1923. [PubMed: 23023588]
30. Bar-Shir A, Liu G, Liang Y, et al. Transforming thymidine into a magnetic resonance imaging probe for monitoring gene expression. J Am Chem Soc. 2013; 135:1617–1624. [PubMed: 23289583]
31. Jamin Y, Eykyn TR, Poon E, Springer CJ, Robinson SP. Detection of the prodrug-activating enzyme carboxypeptidase G2 activity with chemical exchange saturation transfer magnetic resonance. Mol Imaging Biol. 2014; 16:152–157. [PubMed: 23955100]
32. Aime S, Calabi L, Biondi L, De Miranda M, Ghelli S, Paleari L, Rebaudengo C, Terreno E. Iopamidol: exploring the potential use of a well-established x-ray contrast agent for MRI. Magn Reson Med. 2005; 53:830–834. [PubMed: 15799043]
33. Bar-Shir A, Liu G, Greenberg MM, Bulte JW, Gilad AA. Synthesis of a probe for monitoring HSV1-tk reporter gene expression using chemical exchange saturation transfer MRI. Nat Protoc. 2013; 8:2380–2391. [PubMed: 24177294]
34. Bar-Shir A, Liu G, Chan KW, et al. Human protamine-1 as an MRI reporter gene based on chemical exchange. ACS Chem Biol. 2014; 9:134–138. [PubMed: 24138139]
35. Kim M, Gillen J, Landman BA, Zhou J, van Zijl PC. Water saturation shift referencing (WASSR) for chemical exchange saturation transfer (CEST) experiments. Magn Reson Med. 2009; 61:1441–1450. [PubMed: 19358232]
36. Bar-Shir A, Liu G, Liang Y, et al. Transforming thymidine into a magnetic resonance imaging probe for monitoring gene expression. J Am Chem Soc. 2013; 135:1617–1624. [PubMed: 23289583]
37. Zhou J, Lal B, Wilson DA, Laterra J, van Zijl PC. Amide proton transfer (APT) contrast for imaging of brain tumors. Magn Reson Med. 2003; 50:1120–1126. [PubMed: 14648559]
38. Zeger SL, Liang KY. Longitudinal data analysis for discrete and continuous outcomes. Biometrics. 1986; 42:121–130. [PubMed: 3719049]
39. Blasberg RG, Tjuvajev JG. Molecular-genetic imaging: current and future perspectives. J Clin Invest. 2003; 111:1620–1629. [PubMed: 12782662]
40. Iyer M, Sato M, Johnson M, Gambhir SS, Wu L. Applications of molecular imaging in cancer gene therapy. Curr Gene Ther. 2005; 5:607–618. [PubMed: 16457650]
41. Yin W, Xiang P, Li Q. Investigations of the effect of DNA size in transient transfection assay using dual luciferase system. Anal Biochem. 2005; 346:289–294. [PubMed: 16213455]
42. Carnes AE, Williams JA. Plasmid DNA manufacturing technology. Recent Pat Biotechnol. 2007; 1:151–166. [PubMed: 19075838]
43. Iyer M, Wu L, Carey M, Wang Y, Smallwood A, Gambhir SS. Two-step transcriptional amplification as a method for imaging reporter gene expression using weak promoters. Proc Natl Acad Sci U S A. 2001; 98:14595–14600. [PubMed: 11734653]
44. Farrar CT, Buhrman JS, Liu G, Kleijn A, Lamfers ML, McMahon MT, Gilad AA, Fulci G. Establishing the lysine-rich protein CEST reporter gene as a CEST MR imaging detector for oncolytic virotherapy. Radiology. 2015:140251.
45. Song X, Gilad AA, Joel S, et al. CEST phase mapping using a length and offset varied saturation (LOVARS) scheme. Magn Reson Med. 2012; 68:1074–1086. [PubMed: 22246684]
46. Yadav NN, Jones CK, Xu J, Bar-Shir A, Gilad AA, McMahon MT, van Zijl PC. Detection of rapidly exchanging compounds using on-resonance frequency-labeled exchange (FLEX) transfer. Magn Reson Med. 2012; 68:1048–1055. [PubMed: 22837066]
47. Lee JS, Regatte RR, Jerschow A. Isolating chemical exchange saturation transfer contrast from magnetization transfer asymmetry under two-frequency rf irradiation. J Magn Reson. 2012; 215:56–63. [PubMed: 22237631]

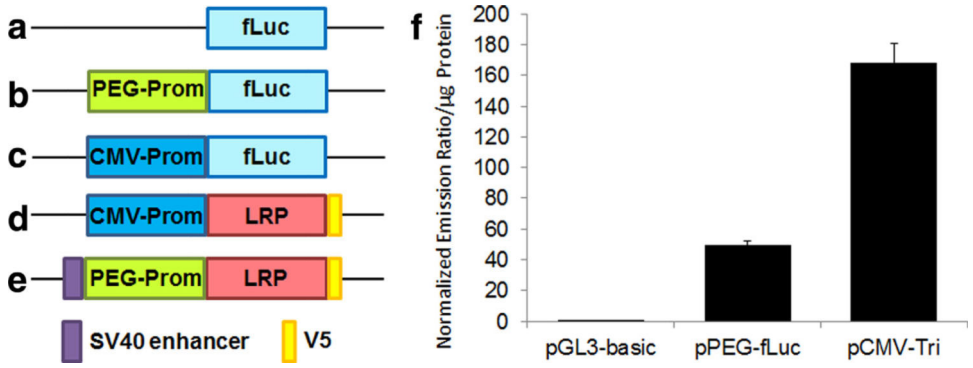

FIG. 1.

a–e: Schematic diagram of the plasmids used. Promoter-less pGL3-basic (**a**), pPEG-fLuc (**b**), pCMV-Tri (showing only the fLuc expression cassette) (**c**), pCMV-LRP (**d**), and pPEG-LRP (**e**). **f**: PEG-3 promoter is active in the rat 9L glioma cell line. Relative activities of PEG-3 promoter and CMV promoter in 9L cells were measured by the dual luciferase assay after transient transfection. Firefly luciferase activity was normalized to that of renilla luciferase and to total protein. Error bars represent standard deviation, n = 3. fLuc: firefly luciferase, V5: V5 tag.

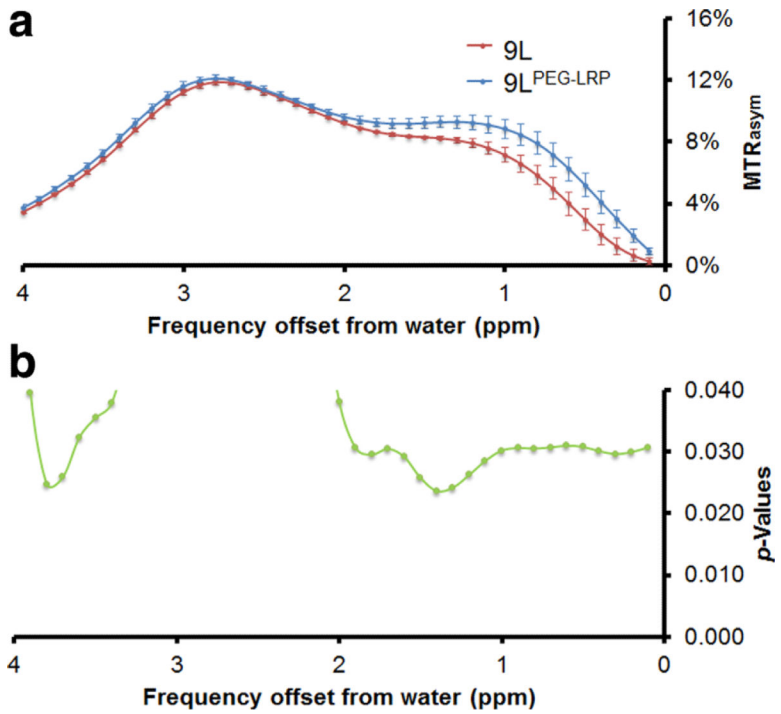

FIG. 2.

9L cells overexpressing LRP generate CEST contrast *in vitro*. Rat 9L glioma cells stably expressing PEG-prom-driven LRP were generated to provide $9L^{PEG\text{-}LRP}$. **a**: *In vitro* CEST contrast in 9L vs. $9L^{PEG\text{-}LRP}$ cells. **b**: The generalized estimating equation (GEE) approach demonstrated a difference in CEST contrast between wild-type and gene-tagged cells at 3.7 ppm, n = 3.

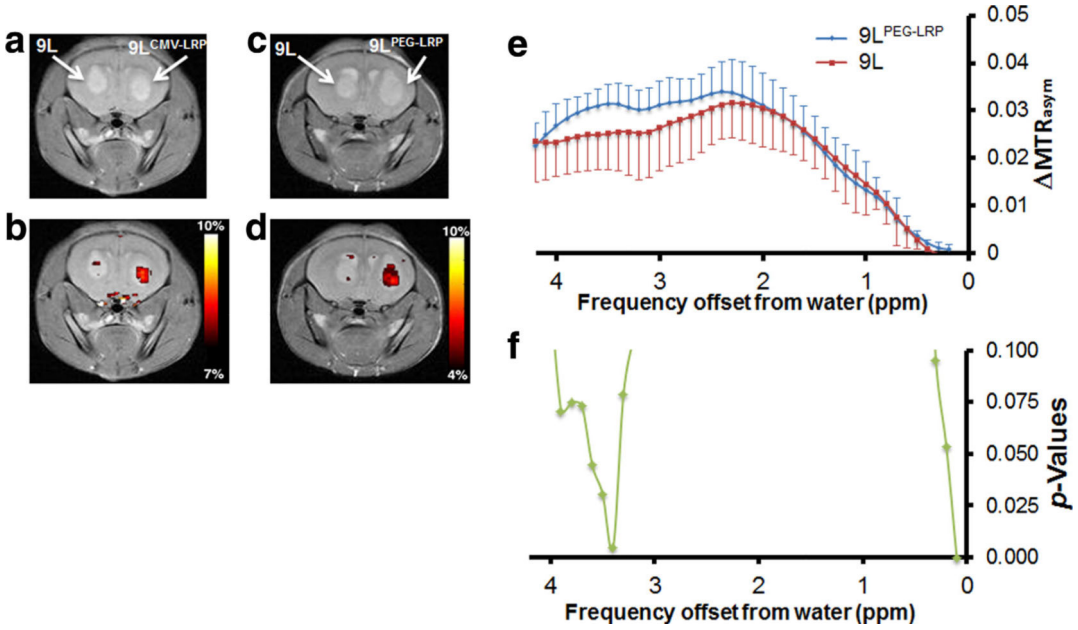

FIG. 3.

PEG-3 promoter:LRP exhibited CEST contrast in a murine model of rat 9L glioma. Representative T2-weighted (**a,c**) and CEST images superimposed on T2-weighted images (**b,d**). The left hemisphere harbors the gene-tagged 9L tumor, namely, CMV-LRP in (a) and (b) and PEG-LRP in (c) and (d), while the right hemisphere has a tumor derived from implantation of wild-type 9L cells. Note that PEG-LRP enables CEST imaging due to the activation of PEG-3 promoter by transcription factors present in the 9L tumor cells. Temporal changes in the ΔMTR_{asym} values of each tumor type (**e**). The generalized estimating equation (GEE) approach demonstrated difference in CEST contrast at 3.4 ppm between tumors derived from wild-type (9L) and gene-tagged ($9L^{PEG\text{-}LRP}$) cells (**f**). The scale in (b and d) is of MTRasym and in (e) the scale is of ΔMTR_{asym}. Mean ± standard deviation; n = 8.